Materials Science-Poland, *Vol. 26*, *No. 1*, *2008*

Technology and properties of GaAs doping superlattices

B. ŚCIANA[1*], D. RADZIEWICZ[1], D. PUCICKI[1], M. TŁACZAŁA[1], G. SĘK[2], P. POLOCZEK[2], J. MISIEWICZ[2], J. KOVÁČ[3], R. SRNANEK[3], A. CHRISTOFI[4]

[1]Faculty of Microsystem Electronics and Photonics, Wrocław University of Technology, ul. Janiszewskiego 11/17, 50-372 Wrocław, Poland

[2]Institute of Physics, Wrocław University of Technology, Wybrzeże Wyspiańskiego 27, 50-370 Wrocław, Poland

[3]Department of Microelectronics, Faculty of Electrical Engineering and Information Technology, Slovak University of Technology, Ilkovičova 3, 812 19 Bratislava, Slovakia

[4]Department of Materials, Imperial College London, London SW7 2AZ, England

Heterojunction and doping superlattices are widely used in many advanced semiconductor devices such as resonant tunnelling diodes, optical modulators, cascade lasers, tunable light emitting diodes and photodetectors. These structures exhibit nonlinear electrooptical properties. Nonlinear processes are governed by the Franz–Keldysh effect and the band-filling effect in the n-i-p-i superlattices and by the quantum-confined Stark effect in the case of n-i-p-i multiple quantum well structures. The paper presents investigations of GaAs n-i-p-i and p-i-p-i doping superlattices grown by atmospheric pressure metal organic vapour phase epitaxy. The properties of the obtained structures were examined using: EC–V method, SIMS spectrometry, photoluminescence and photoreflectance spectroscopy.

Key words: *doping superlattice; δ-doping; AP MOVPE; photoreflectance, photoluminescence*

1. Introduction

Unique properties of doping superlattices include a superlattice energy gap smaller than the gap energy of the bulk semiconductor, spatial separation of electron and hole wave functions, and smaller oscillator strength of optical transitions. These features are responsible for a prolongation of the carrier lifetime and a large reduction in the absorption coefficient [2]. Thus, doping superlattices are very attractive for application in tunable optoelectronic devices. Semiconductor doping superlattices are mainly fabricated by two epitaxial methods: molecular beam epitaxy (MBE) and metal organic

*Corresponding author, e-mail: Beata.Sciana@pwr.wroc.pl

vapour phase epitaxy (MOVPE). Employment of the δ-doped technique [3, 4] results in a spatial confinement of dopants to a single atomic plane. The paper presents the technology and properties of GaAs-based n-i-p-i and p-i-p-i superlattices deposed by atmospheric pressure metal organic vapour phase epitaxy (AP MOVPE). Various methods used for determination the spatial localisation of dopants and optical properties of the investigated structures are presented and discussed.

2. Experiment

The GaAs n-i-p-i and p-i-p-i doping superlattices were grown by AP MOVPE on (100)-oriented semi-insulating GaAs substrate, using an AIX 200 R&D Aixtron horizontal reactor. TMGa, AsH_3 (10% mixture with H_2), SiH_4 (20 ppm mixture with H_2) and DEZn were used as the growth and dopant precursors. High purity hydrogen was employed as a carrier gas. A δ-doping procedure "purge-doping-purge" was applied for formation of the n-type and p-type delta-doped regions. The n-i-p-i structure consisted of the alternating p-type (Zn) and n-type (Si) δ-doped regions, separated by 50 nm of undoped GaAs (periodicity: z_0 = 100 nm). The structure consisted of 5.5 periods. Designed sheet donor and acceptor concentrations were $N_A^{2D} = N_D^{2D} \approx 1\times10^{12}\,\mathrm{cm}^{-2}$. The p-i-p-i structure consisted of 10 of the p-type (Zn) δ-doped regions separated by 15 nm of undoped GaAs (periodicity: z_0 = 15 nm). The designed sheet acceptor concentration was $N_A^{2D} \approx 1\times10^{12}\,\mathrm{cm}^{-2}$. The thickness of the top undoped GaAs layer was 20 nm. For example the epitaxial structure, the scheme of the doping profile and the band diagram of the designed n-i-p-i structure are shown in Figs. 1, 2. AP MOVPE processes were carried out at 650 °C (n-i-p-i) and at 670 °C (p-i-p-i) under optimal growth conditions, estimated from earlier studies [5, 6].

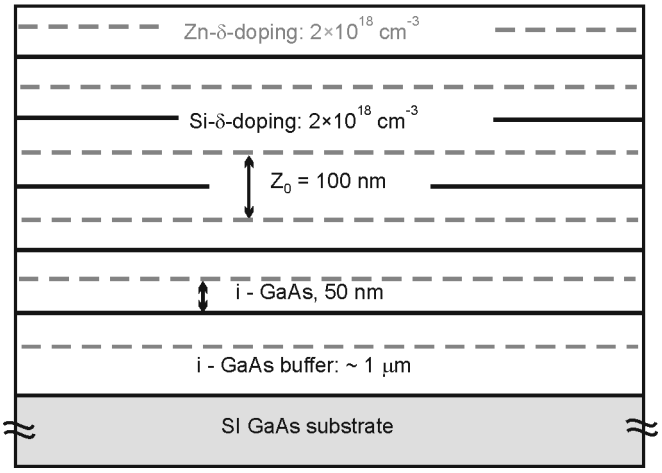

Fig. 1. Epitaxial structure of the n-i-p-i GaAs superlattice

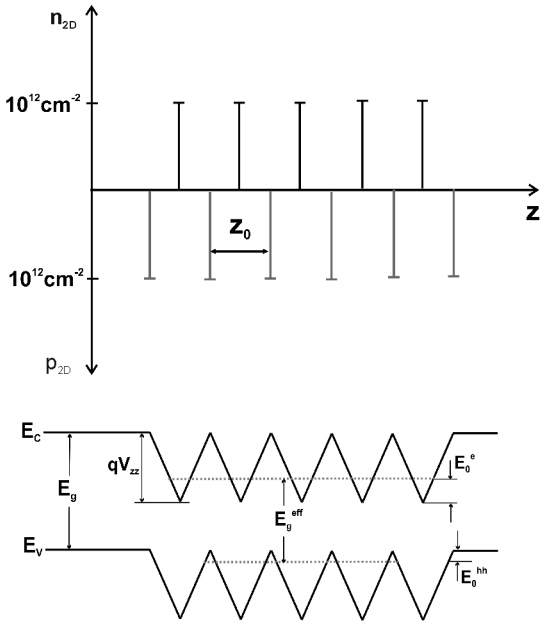

Fig. 2. Scheme of the doping profile and the band diagram of the designed n-i-p-i GaAs superlattice

3. Results and discussion

3.1. Electrochemical capacitance–voltage measurements

The carrier distribution across the investigated structures was measured using a Bio-Rad PN 4300 electrochemical capacitance–voltage (EC–V) profile at the frequency of 3 kHz. The method applies the capacitance–voltage analysis of a reverse bias electrolyte–semiconductor Schottky diode for evaluation of a free carrier concentration. The EC–V profiles of the n-i-p-i and p-i-p-i structures are presented in Figs. 3 and 4, respectively.

In the case of the long period n-i-p-i superlattice 6 spikes connected with the p-type δ-doped regions are visible. The best accuracy is obtained for the first peak with the maximum hole concentration of 5×10^{18} cm^{-3} and the width of 6 nm. The distance between p-type doped regions is about 85 nm ($< z_0 = 100$ nm). Next spikes exhibit lower hole concentrations and a significant profile broadening due to the influence of the etch non-uniformity and a large series resistance [7]. The presence of free carriers indicates that the n-i-p-i structure is not fully compensated (sample has got 6 p-type regions and 5 n-type regions). For a short period p-i-p-i structure, large EC–V profile broadening is observed, thus determination of the carrier concentration and localisation in the p-type δ-doped regions is impossible.

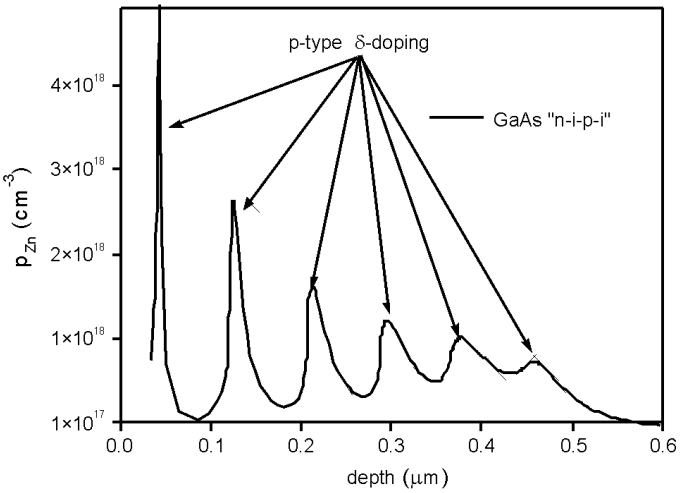

Fig. 3. Electrochemical capacitance-voltage profile of the n-i-p-i superlattice

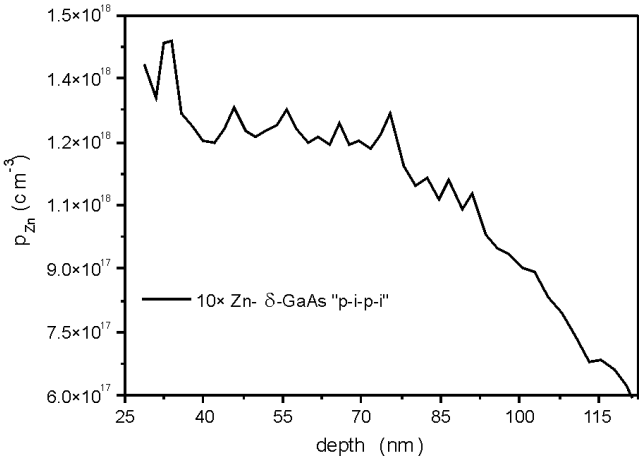

Fig. 4. Electrochemical capacitance-voltage profile of the p-i-p-i superlattice

3.2. Secondary ion mass spectrometry

Secondary ion mass spectrometry (SIMS) was applied for determination of the dopant distribution in the investigated structures. In contrast to the C–V profiling based on a free carrier effect, this method gives information about dopant atoms. The SIMS profiles of the n-i-p-i and p-i-p-i structures are shown in Figs. 5 and 6, respectively. All clearly resolved peaks connected with Zn and Si atoms localised in the δ-doped regions are visible in the figures. The superlattice period of 100 nm and

15 nm was estimated for the n-i-p-i and p-i-p-i structure, respectively, what corresponds very well to the designed values.

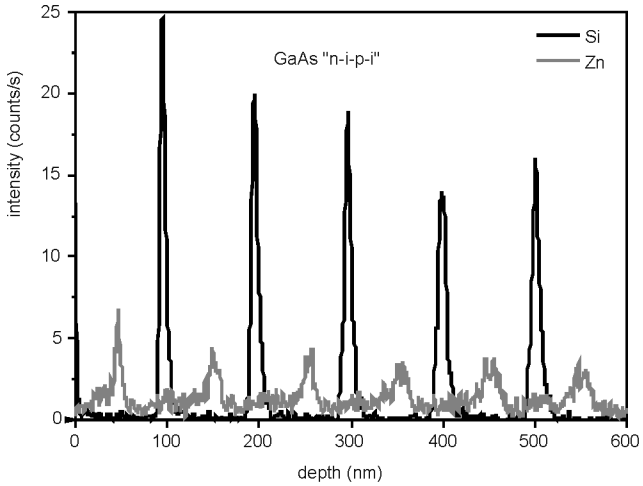

Fig. 5. SIMS profile of the n-i-p-i superlattice

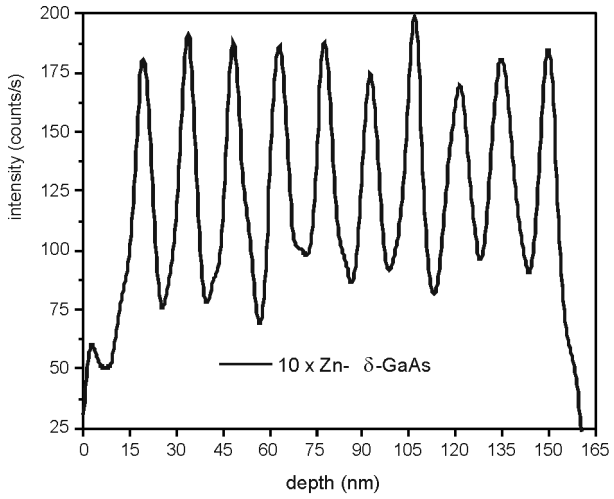

Fig. 6. Secondary ion mass spectrometry profile of the p-i-p-i superlattice

In Figure 5, the width of the SIMS peaks increases (6–9 nm for Si and 8–17 nm for Zn) upon the depth what could be connected with increasing the roughening of the sputtered crater with the sputtering time. In the case of deeper localised Zn atoms, the broadening can be also explained by diffusion. The SIMS profile of the p-i-p-i structure shown in Fig. 6 exhibits nearly the same peak width (9–10 nm). This structure is much thinner than the n-i-p-i superlattice, so both the growth and the sputtering times were shorter in this case.

3.3. Photoluminescence and photoreflectance measurements

Photoreflectance (PR) spectroscopy was applied for determination of the energy band structure of the doping superlattices. The method is a classical modulation spectroscopy. An internal electric field of the investigated material is modulated with an absorbed laser beam and the photoinduced changes in the reflectance spectrum are measured, yielding a derivative-like spectral response with a high sensitivity to optical transitions. Photoreflectance was measured using a 150 W tungsten halogen lamp as a probe beam source and 632.8 nm line of He-Ne laser as the pump beam, which was mechanically chopped at 275 Hz. Further details of the experimental PR set-up have been described elsewhere [8].

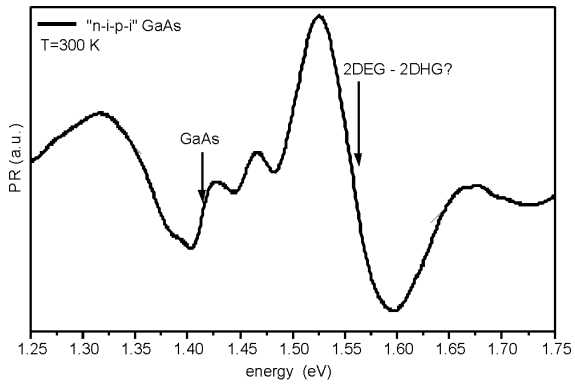

Fig. 7. Photoreflectance spectrum of the n-i-p-i superlattice

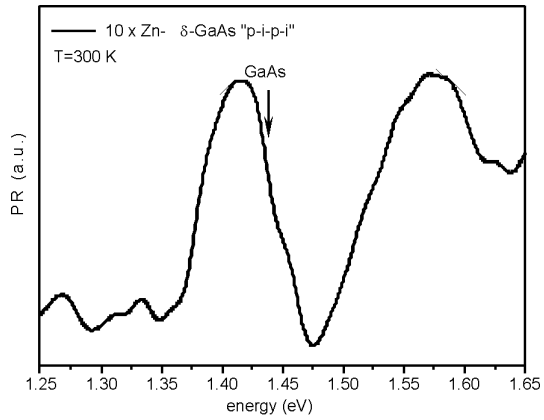

Fig. 8. Photoreflectance spectrum of the p-i-p-i superlattice

PR spectra of the n-i-p-i and p-i-p-i structures recorded at 300 K are shown in Figs. 7 and 8, respectively. PR spectrum of the n-i-p-i superlattice (Fig. 7) exhibits two optical transitions. The first weak transition at 1.42 eV is connected with the band-gap energy of GaAs (the undoped parts of the structure) and the second strong transition at 1.56 eV is

unusual for the bulk GaAs and comes probably from the transitions involving two-dimensional electron gas and two-dimensional hole gas. In the PR spectrum of the p-i-p-i structure (Fig. 8) the transition related to the band-gap energy of GaAs and some Franz –Keldysh oscillations (FKO) for higher energies are visible. FKO oscillations come from an internal electric field introduced by ionised Zn δ-doped centres.

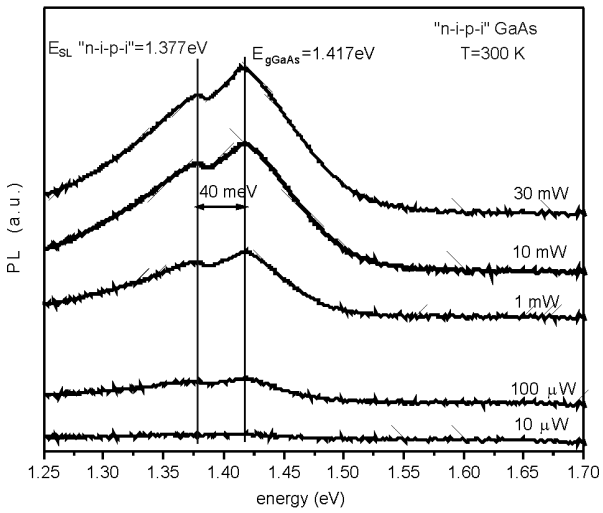

Fig. 9. Photoluminescence spectra of the n-i-p-i superlattice

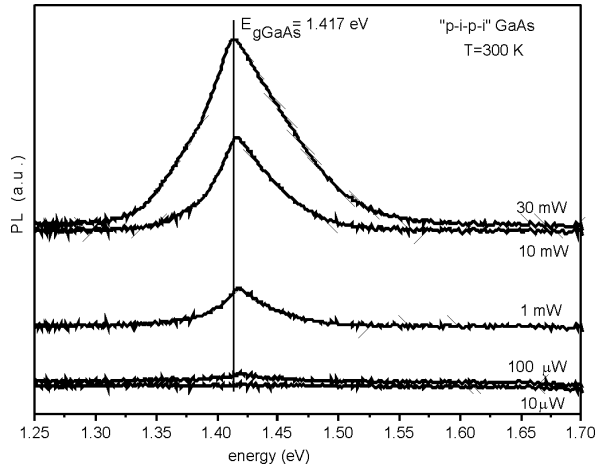

Fig. 10. Photoluminescence spectra of the p-i-p-i superlattice

Photoluminescence (PL) spectroscopy is an emission-like experiment giving information about various radiative recombination channels in semiconductors. PL spectra of the investigated structures were recorded using a standard experimental configuration with 532 nm line of a frequency doubled Nd:YAG laser as the excitation source,

and a cooled InGaAs PIN photodiode combined with 0.55 m focal length monochromator as the detection system. PL spectra of the n-i-p-i and p-i-p-i structures recorded at 300 K for various optical excitation intensities (10 μW–30 mW) are shown in Figs. 9 and 10, respectively. For the n-i-p-i structures (Fig. 9) beside the emission line related to the band-gap of GaAs (1.417 eV), an additional PL peak is visible at 1.377 eV. It is probably connected with subband transitions inside the V-shaped potential wells and corresponds to the effective band gap of the sawtooth n-i-p-i superlattice. The energy of this peak does not change upon variation of the excitation intensity. In the case of the p-i-p-i structure (Fig. 10), free carriers (holes) screen their parent ionised acceptors and only one PL peak related to band-gap of GaAs is observed.

4. Conclusions

The technology and properties of GaAs-based n-i-p-i and p-i-p-i superlattices are presented and discussed. The results of EC–V measurements indicate that in the case of multi-δ-doped structures, a precise determination of the carrier concentration in each δ-layer is impossible due to the etch non-uniformity and a large series resistance. For a short period superlattices the method is useless. Accurate localisation of Zn and Si atoms in δ-doped regions was possible by applying the SIMS technique. The SIMS profiles of the p-i-p-i superlattices indicate that AP MOVPE technology allows one to obtain a short period (z_0 = 15 nm) doping superlattice using Zn dopant. The optical transitions related to the sawtooth superlattice are visible in the PR and PL spectra of the long period n-i-p-i structures.

Acknowledgements

This work was partially supported by the Wrocław University of Technology statutory grant, the Ministry of Scientific Research and Information Technology, grant No. 515 002 31/0239, and by a bilateral cooperation Pol/Slov project.

References

[1] ANDO H., IWAMURA H., OOHASHI H., KANABE H., IEE J. Quant. Electr., 26 (1989), 2135.
[2] SCHUBERT E.F., HORIKOSHI Y., PLOOG K., Phys. Rev., 36 (1985), 1085.
[3] SCHUBERT E.F., J. Vac. Sci. Technol. A, 8 (1990), 2980.
[4] LI G., JAGADISH C., Solid-State Electr., 41 (1997), 1207.
[5] ŚCIANA B., RADZIEWICZ D., PUCICKI D., TŁACZAŁA M., SĘK G., Proc. of the 5th Intern. EuroConference ASDAM 2004, October 2004, Smolenice, Slovakia, pp. 111–113.
[6] ŚCIANA B., RADZIEWICZ D., PASZKIEWICZ B., TŁACZAŁA M., SITAREK P., SĘK G, MISIEWICZ J., KINDER R., KOVAC J., SRNANEK R., Thin Solid Films, 412 (2002), 55.
[7] SELL B., GATZKE C., FERNÁNDEZ J.M., Semicond. Sci. Technol., 13 (1998), 423.
[8] MISIEWICZ J., SĘK G., KUDRAWIEC R., SITAREK P., Thin Solid Films, 450 (2004), 14.

Received 28 April 2007
Revised 16 February 2008